# Hole opening from growing interfacial voids: A possible mechanism of solid state dewetting

Stefano Curiotto, Anna Chame, Pierre Müller, Carl Thompson, Olivier Pierre-Louis

# Hole opening from growing interfacial voids: A possible mechanism of solid state dewetting

Stefano Curiotto,[1] Anna Chame,[2] Pierre Müller,[1] Carl V. Thompson,[3] and Olivier Pierre-Louis[4]
[1)]*Aix Marseille Univ, CNRS, CINAM, AMUTECH, Marseille, France*
[2)]*Instituto de Física, Univ. Federal Fluminense, Avenida Litorânea s/n, 24210-340 Niterói RJ Brazil*
[3)]*Department of Materials Science and Engineering, Massachusetts Institute of Technology, USA*
[4)]*Institut Lumière Matière, UMR 5306 Université Lyon 1-CNRS, Universitè de Lyon, 69622 Villeurbanne, France*

(*Author to whom correspondence should be addressed: Stefano Curiotto: stefano.curiotto@cnrs.fr)

(*Anna Chame: achame@id.uff.br)

(*Pierre Müller: pierre.muller@univ-amu.fr)

(*Carl V. Thompson: cthomp@mit.edu)

(*Olivier Pierre-Louis: olivier.pierre-louis@univ-lyon1.fr)

Vacancies at interfaces between a film and a substrate can affect material properties and could play a role in solid state dewetting. Using Kinetic Monte Carlo simulations, we show that interfacial mono-vacancies diffuse and coalesce to form vacancy clusters and voids. The film/substrate excess energy $E_S$ which is related to the apparent contact angle controls the mechanisms of coalescence. Depending on $E_S$, voids emerging at the film surface form a hole that can be filled by the film or can lead to the dewetting of the film from the substrate.

Mono-vacancies in solid materials can coalesce and form vacancy clusters and voids that significantly impact material properties and stability. The size and the distribution of the vacancy clusters not only affect the mechanical properties of a material[1] but also optical and electric properties[2] and are therefore important for material applications. With the development of nanotechnologies and the size reduction of devices, the importance of the evolution of vacancy clusters has further increased[3]. Our work is mainly motivated by the need for a better understanding of the stability of thin films. Thin solid films deposited on a substrate are often unstable and tend to break-down and agglomerate into 3D isolated particles, through a phenomenon called solid state dewetting (SSD)[4]. On one hand, SSD leads to important morphological changes of a film and can thus make devices inoperative, and strategies to limit this phenomenon must therefore be developed[5]. On the other hand, SSD can be used to form organized patterns of particles on surfaces[6–8], for instance to exploit optical properties[9]. While in polycrystalline films SSD starts at grain boundaries, the origin of SSD in single crystal films, such as Silicon on Insulator (SOI) films[10–12], is less clear. As suggested by Shaffir, Riess and Kaplan[13], interfacial mono-vacancies can coalesce and form voids that grow and lead to SSD. Studying the agglomeration of Au films deposited on $SiO_2$, Kwon et al. propose that SSD can be due to voids, formed by vacancy coalescence, that grow at the substrate/film interface[14]. Vacancies can be formed during the deposition of the thin film or they can appear at later stages, for instance under strain[15], or when the material is heated in order to partially relax interface stress[16]. Vacancies can also form from defects, grain boundary junctions with the substrate, or film edges and diffuse at the film/substrate interface. They can therefore play an important role in patterned films that present many edges as in Refs. 9 and 17. Our simulations show that mono-vacancies and vacancy clusters at the interface can coalesce and form voids. When these voids are large enough, they emerge at the film surface and can sometimes lead to dewetting, depending on the wetting properties of the film.

As an interface is surrounded by different materials and thus is not freely accessible, experimental studies of interfacial vacancies and of their coalescence are difficult. Atomistic simulations are thus a convenient tool to investigate these processes. Kinetic Monte Carlo (KMC) simulations based on the solid-on-solid (SOS) method, that forbids overhangs, have been shown to predict many features of solid state dewetting[18–21]. SOS simulations are fast, but do not allow study of vacancies at interfaces or in the bulk. In this work we have used a 3D KMC code similar to that of Ref. 22, with atoms on a Hexagonal Close Packed (HCP) lattice. Atoms can jump to unoccupied neighboring sites with rates proportional to $\exp[-(nJ - E_S\delta_S)/(kT)]$, where $n$ is the number of nearest neighbors, $J$ is a binding energy (taken as the energy unit in the following), $k$ is the Boltzmann constant and $T$ is the temperature. $E_S$ is the film/substrate excess energy and defines the wetting properties between the substrate and the film, and $\delta_S = 1$ for atoms that are in contact with the substrate and $\delta_S = 0$ otherwise. Atoms can only move to sites where they have neighbors, i.e. on the top surface, on the substrate, and in regions within voids, but they cannot detach from the film or from the substrate. For convenience and using an analogy with the isotropic case (for instance a liquid droplet on a surface), an apparent void wetting angle $\theta$ can be defined using $E_S$ as $\theta = \arccos(\frac{E_S}{\gamma_f} - 1)$, where $\gamma_f$ is the surface energy of the (0001) film (notice that the film/substrate wetting angle $\theta'$ is related to $\theta$: $\theta' = 180 - \theta$). In the simulations, $E_S$ is fixed to a value between 0 (complete wetting limit) and $3J$ (strong dewetting tendency). Additional details on the model and on the relation between $E_S$ and the wetting properties are provided in the supplementary material.

Let us start with a description of the early stages of the dy-

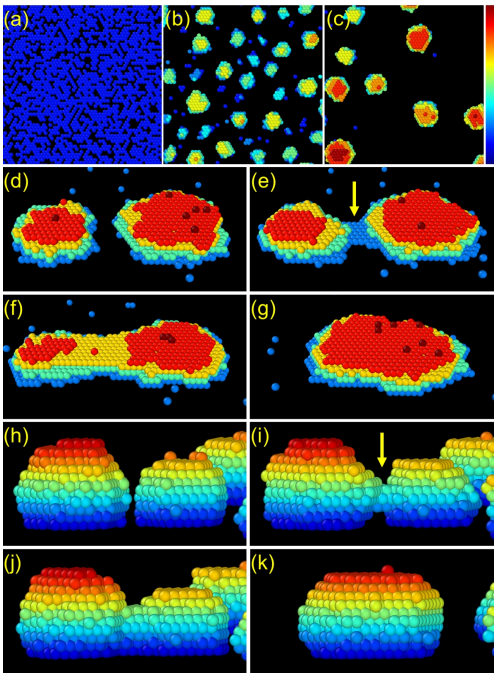


FIG. 1. Growth of vacancy clusters. (a) View from below the film-substrate interface (from the substrate to the film) at the beginning of the simulation, with a fixed number of interfacial vacancies (the blue spots, 68% of the sites). (b): after some time, the vacancies have coalesced and formed several 3D vacancy clusters. (c): at longer times the vacancy clusters also have coalesced and have formed larger voids. (d-g): perspective view from above the film-substrate interface of the coalescence of two voids for $E_S = 2.5J$ (poor film/substrate adhesion), $kT = 0.6J$. In (d) the voids are well separated. In (e) a 2D bridge of interfacial empty sites shown by the yellow arrow has formed between the voids. (f): the 2D bridge in (e) has become a 3D tunnel. The coalescence is complete in (g), where the two voids have merged in a larger void. (h-k) coalescence of two voids for $E_S = 0.5J$ (good film/substrate adhesion), $kT = 0.6J$. In this case the bridge of empty sites is formed in the bulk of the film, at about half the height of the voids (see the arrow). The colored spheres are empty sites, atoms are not represented. Empty sites at the film/substrate interface are blue, those on the top of the voids are dark red (the color scale is represented on the top-right of the image). In (d-g) the dark red empty sites are in the $5^{th}$ layer, while in (h-k) they are in the $11^{th}$ layer. The in-plane size of the simulation box is 100×100 atomic positions.

namics. As an initial condition for the simulations, we use a fixed concentration of empty sites at the interface. For all values of $E_S$, as the system evolves in time, the vacancies diffuse and coalesce at the interface forming vacancy clusters and voids. A bottom view of the evolution of the system is shown in Figure 1(a,b,c). As a result of atom hopping, vacancy clusters and voids move randomly at the interface and can also diffuse to upper layers. They coalesce and form 2D (i.e., monolayer) and 3D (i.e., multilayer) voids in contact with the substrate (see figures 1b and 1c, and movies 1 and 2 in the supplementary material). The increase in the average void size is more due to coalescence than to Ostwald-ripening coarsening. As shown in[23], at low temperature the diffusion of mono-vacancies at interfaces is slower than the diffusion of 2D vacancy clusters. However, the diffusion coefficient of 2D vacancy clusters decreases for larger sizes, where universal scaling applies[24–27]. We expect that the mobility of 3D vacancy clusters will behave in a similar way as a function of size. In addition, it is also known that the diffusion constants of atom clusters and vacancy clusters exhibit an oscillatory dependence on their size[23,26,28]. These combined effects are expected to lead to a complex dependence of the diffusion coefficient on size.

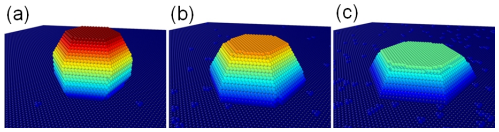


FIG. 2. Equilibrium shape of voids at a film/substrate interface with $E_S$= 0.5, 1.5, 2.5$J$ from (a) to (c). The number of interfacial mono-vacancies increases from (a) to (c). $kT = 0.1J$. The in-plane size of the simulation box is 200×200. The figures show the atoms surrounding the voids, therefore three blue atoms at the interface indicate the presence of an interfacial mono-vacancy. The dark blue atoms are on the substrate, while the dark red atoms are in layer 24.

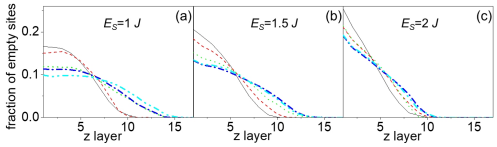


FIG. 3. Fraction of empty sites as a function of the film layer (layer 1 is on the substrate, layer 20 is the film surface). $E_S$=1, 1.5 and 2$J$ for (a), (b) and (c) respectively, kT=0.9$J$. The in-plane size of the simulation box is 200×50. The initial fraction of empty sites, not represented in the figure, is the same for all values of $E_S$. At the beginning of the simulations, the empty sites are all in the first layer, in contact with the substrate. Curves with different colors are taken at different times (see the supplementary material for the exact times) in the following order: thin black line, red dashes, green dots, dark blue dash-dot, light blue dash dot dot. At large times, the number of empty sites close to the substrate decreases and that of empty sites in upper layers increases, but the total number of empty sites is conserved at all times. This change is more important at low $E_S$. Curves with the same color are taken after the same number of time steps in (a), (b) and (c).

Due to their random diffusive motion, voids meet and coalesce to form larger and larger voids, as shown in figure 1(d-k). This process is similar to the coalescence of droplets[29].

The dynamics of the reshaping of the two merging voids, also called sintering, has been described in the literature[26]. Here, we notice that two distinct scenarios can be observed as a function of $E_S$. For large $E_S$ (i.e. poor film/substrate adhesion), the void coalescence takes place with the formation of a 2D bridge of empty sites at the film/substrate interface between the two voids, as shown in figure 1e. For longer times, the 2D bridge becomes 3D (see figure 1f), and the voids evolve toward a more compact equilibrium shape to reduce the total surface energy (figure 1g). For small $E_S$ (i.e. good film/substrate adhesion), the initial bridge of empty sites does not form at the film/substrate interface but in the bulk, as shown in figures 1h-k.

We observe that the average vacancy-cluster size increases faster for larger $E_S$ (see movies 1 and 2 in the supplementary material). Some hints about the dependence of size-increase speed with $E_S$ can be gained by an inspection of the equilibrium shape of a single void, shown in Fig. 2. Indeed, we observe that: (i) the triple line at the edge of the void fluctuates more and faster for high $E_S$. This could be related to the larger number of interfacial mono-vacancies at the interface, as seen in Fig. 2(c) for large $E_S$. In addition, the hopping rate of adatoms on the substrate is higher when $E_S$ is larger. As a second observation, (ii) the projected area of a void on the substrate is larger for high $E_S$ (for a given volume) and thus the probability of meeting another void is larger than for small $E_S$.

Figure 3a shows the number of empty sites in the film as a function of the distance from the substrate for $E_S = 1.0J$ for different times. For all values of $E_S$, the fraction of empty sites spreads and reaches layers that are more distant from the substrate as time increases. For large $E_S$ (see figures 3b and 3c) the curves are steeper. Indeed, the equilibrium height of voids is smaller for large $E_S$. In addition, the total number of empty sites in the voids, i.e. the total volume of the voids, is smaller at large $E_S$ due to the presence of a large number of mono-vacancies at the interface.

In thin films, the coalescence of voids may lead to voids that are large enough to emerge at the film surface, thus making a hole in the film. The ultimate fate of this hole depends on $E_S$. In order to investigate this process, we have performed simulations starting with only one void in its equilibrium shape in a film with a flat surface which was one layer higher than the void height. Due to thermal fluctuations, the thin film layer above the void breaks down and a hole forms. Movie 3 in the supplementary material and figures 4a, 4b, 4d, 4e show an example of dynamics of hole formation, for $E_S = 0.5J$. Letting the system evolve further for $E_S = 0.5J$, the film fills the hole and the void disappears, leaving a depression at the film surface (see figures 4c and 4f). This depression is smoothed away if the simulation is continued, and the total film height decreases. In contrast, when $E_S = 2.5J$, the hole formed by the void is not filled and dewetting occurs. This is followed by the standard scenario for dewetting, with the formation of a rim around the hole, as shown in figures 4g-l (see also movie 4 in the supplementary material). In general, we find that dewetting starts approximately when $E_S > 1.5J$.

If the void is covered by more than one layer ($\Delta$h in the insert of figure 5a), then the value of $E_S$ required to observe dewetting increases. Using a film thinner than the equilibrium void height (negative $\Delta$h), the initial condition corresponds to a void truncated by the film surface. In these cases, a smaller value of $E_S$ is sufficient to make the film dewet. Figure 5a shows the difference between the thickness of the film and the void height as a function of $E_S$ for different void volumes. Voids with different volumes behave differently and larger voids (red circles in figure 5a) lead more easily to dewetting. Interestingly, rescaling the height $\Delta$h with the characteristic size of the void volume (i.e. $\Delta h \propto N^{1/3}$, with $N$ the number of empty sites in the void) does not lead to the collapse of these curves (see figure 5b). This absence of collapse is probably caused by the relevance of another length-scale related to surface fluctuations (such as those that can be built using surface tension and the lattice parameter).

To summarize, we have shown that diffusing interfacial vacancies coalesce, leading to voids that also diffuse and grow in size, mainly by coalescence. In single crystal thin films, such voids can emerge at the film surface and form a hole that initiates solid state dewetting, particularly when the wetting between the film and the substrate is poor. The transition occurs roughly for $E_S$ around 1.5 $J$, i.e. for apparent contact angles of about 90 degrees. Interestingly, in systems with a small apparent contact angle $\theta'$, i.e. $E_S$ smaller than 1.5 $J$ and large $\theta$, the film can fill small holes resulting from the emergence of voids and annealing could therefore lead to the removal of interfacial vacancies from the film/substrate interface without breaking/dewetting the film. In addition, voids can also be formed at defects or generated by strain[16,30,31]. Our KMC model is based on a rigid lattice, and the total number of empty sites is strictly conserved. In some materials, small vacancy clusters can collapse into dislocation loops[32] or stacking fault tetrahedra[33]. However, once a growing void is large enough, this collapse becomes unlikely, owing to the large energy barrier associated with the conversion process[32]. In addition, extended defects such as dislocations[34,35], or grain boundaries[30,31] could act as sinks or sources of vacancies and play an important role in the growth of voids. A perspective of our work is to use other simulation techniques to compare quantitatively the stability of voids with respect to other defects and to evaluate the effect of non-conservation of the number of vacancies. Our results open new directions for experimental and theoretical investigations of void dynamics at interfaces and of the initial stages of solid-state dewetting. Another important perspective of our work is to understand if the criterion of a critical apparent wetting angle around 90 degrees can also be experimentally observed or has to be modified when vacancies are initiated by defects or strain.

## SUPPLEMENTARY MATERIAL

The supplementary material shows details on the KMC model; the relation between $E_S$ and the wetting properties; the change of void shape with temperature; two movies of the vacancy-cluster diffusion and coalescence for $E_S$=0.5 and 2.5 $J$; and two movies on how voids can form holes in the film,

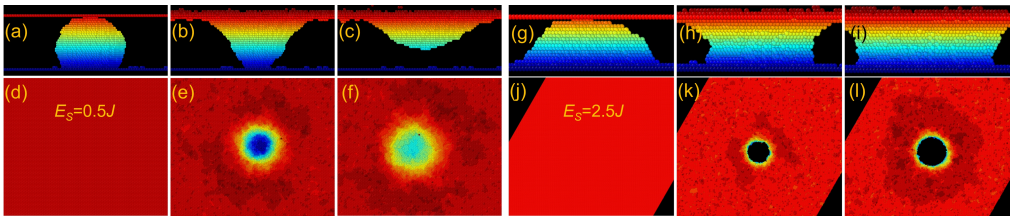


FIG. 4. Dewetting or not dewetting from a void emerging at the surface. When $E_S$=0.5, kT=0.9$J$ (a-c lateral views and d-f corresponding top views), a hole initially formed in the film (b). However, at longer times, the hole is filled (it appears to detach from the film-substrate interface) and a depression at the film surface is left (c). When $E_S$=2.5, kT=0.9$J$ (g-i), the hole increases in size, dewetting starts and the height of the rim formed around the hole increases (dark red atoms). Colors represent atoms surrounding the vacancy cluster or atoms at the film surface, at distances from the substrate, as shown in the color scale of figure 1. The in-plane size of the simulation box is 200×200.

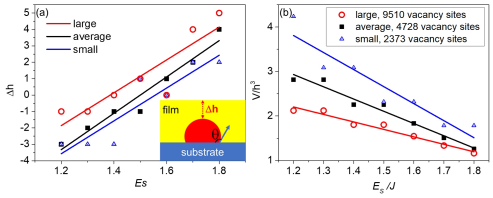


FIG. 5. Transition to dewetting. (a) Critical difference between the film thickness and the void height (Δh) as a function of $E_S$. The symbols indicate the largest thickness (in terms of Δh) for which the hole created by a void will start dewetting for a given $E_S$. Results are plotted for void sizes 9510, 4728 and 2373 (number of empty sites). The in-plane size of the simulation box is 200×200, the film heights at $E_S$=1.5$J$ and Δh=0 are 18, 15 and 10. $kT$=0.9$J$. The inset illustrates the definition of the apparent void contact angle $\theta$ and Δh. (b) The volume of the void leading to dewetting at a given film height $h$ is divided by $h^3$ and plotted as a function of $E_S/J$. The three curves are not superposed, showing that the height of the film is not the only length-scale involved in the dynamics.

and lead (or not) to dewetting.

## ACKNOWLEDGMENTS

We are grateful to M. A. L'Etoile and Y. A. Shin for interesting discussions.

## DATA AVAILABILITY

The data that support the findings of this study are available from the corresponding author upon reasonable request.

## REFERENCES

[1]J. A. Hudson, E. Liu, and S. Crampin, Geophysical Journal International **124**, 105 (1996).
[2]I. V. Kityk, B. Marciniak, and A. Mefleh, Journal of Physics D: Applied Physics **34**, 1 (2001).
[3]F. Wang, Y. Dai, and J. Zhao, Superlattices and Microstructures **100**, 237 (2016).
[4]C. V. Thompson, Annual Review of Materials Research **42**, 399 (2012).
[5]F. Leroy, L. Borowik, F. Cheynis et al., Surface Science Reports **71**, 391 (2016).
[6]M. Trautmann, F. Cheynis, F. Leroy et al., Applied Physics Letters **110**, 263105 (2017).
[7]M. Trautmann, F. Cheynis, F. Leroy, S. Curiotto, and P. Müller, Applied Physics Letters **110**, 161601 (2017).
[8]J. Ye and C. V. Thompson, Advanced Materials **23**, 1567 (2011).
[9]M. Naffouti, T. David, A. Benkouider et al., Small **12**, 1 (2016).
[10]F. Cheynis, E. Bussmann, F. Leroy, T. Passanante, and P. Müller, Physical Review B **84** (2011).
[11]E. Bussmann, F. Cheynis, F. Leroy, P. Müller, and O. Pierre-Louis, New Journal of Physics **13**, 043017 (2011).
[12]S. Curiotto, F. Leroy, F. Cheynis, and P. Müller, Applied Physics Letters **104**, 061603 (2014).
[13]E. Shaffir, I. Riess, and W. Kaplan, Acta Materialia **57**, 248 (2009).
[14]J.-Y. Kwon, T.-S. Yoon, K.-B. Kim, and S.-H. Min, Journal of Applied Physics **93**, 3270 (2003).
[15]D. Tanguy, Phys. Rev. B **96**, 174115 (2017).
[16]W. Gruber, S. Chakravarty, C. Baehtz et al., Phys. Rev. Lett. **107**, 265501 (2011).
[17]M. Abbarchi, M. Naffouti, B. Vial et al., ACS Nano **8**, 11181 (2014).
[18]O. Pierre-Louis, A. Chame, and Y. Saito, Physical Review Letters **99**, 136101 (2007).
[19]O. Pierre-Louis, A. Chame, and Y. Saito, Physical Review Letters **103**, 195501 (2009).
[20]O. Pierre-Louis, A. Chame, and M. Dufay, The European Physical Journal B **77**, 57 (2010).
[21]A. Chame, Y. Saito, and O. Pierre-Louis, Physical Review Materials **4**, 094006 (2020).
[22]O. Pierre-Louis and Y. Saito, EPL (Europhysics Letters) **86**, 46004 (2009).
[23]S. Curiotto, P. Müller, F. Cheynis, and F. Leroy, Applied Surface Science **552**, 149454 (2021).
[24]K. Binder and M. H. Kalos, Journal of Statistical Physics **22**, 363 (1980).
[25]S. V. Khare, N. C. Bartelt, and T. L. Einstein, Physical Review Letters **75**, 2148 (1995).
[26]K. C. Lai, Y. Han, P. Spurgeon et al., Chemical Reviews **119**, 6670 (2019).
[27]F. A. Nichols, Journal of Nuclear Materials **30**, 143 (1969).
[28]M. Ignacio and O. Pierre-Louis, Phys. Rev. B **86**, 235410 (2012).
[29]P. Meakin, Reports on Progress in Physics **55**, 157 (1992).
[30]D. Hull and D. Rimmer, Philosophical Magazine **4**, 673 (1959).
[31]M. Upmanyu, D. J. Srolovitz, L. Shvindlerman, and G. Gottstein, Interface Science **6**, 289 (1998).
[32]S. J. Zinkle, L. E. Seitzman, and W. G. Wolfe, Philosophical Magazine **51**, 111 (1987).

[33] B. Uberuaga, R. Hoagland, A. Voter, and S. Valone, Physical review letters **99**, 135501 (2007).

[34] V. Lubarda, M. Schneider, D. Kalantar, B. Remington, and M. Meyers, Acta Materialia **52**, 1397 (2004).

[35] S. Traiviratana, E. M. Bringa, D. J. Benson, and M. A. Meyers, Acta Materialia **56**, 3874 (2008).

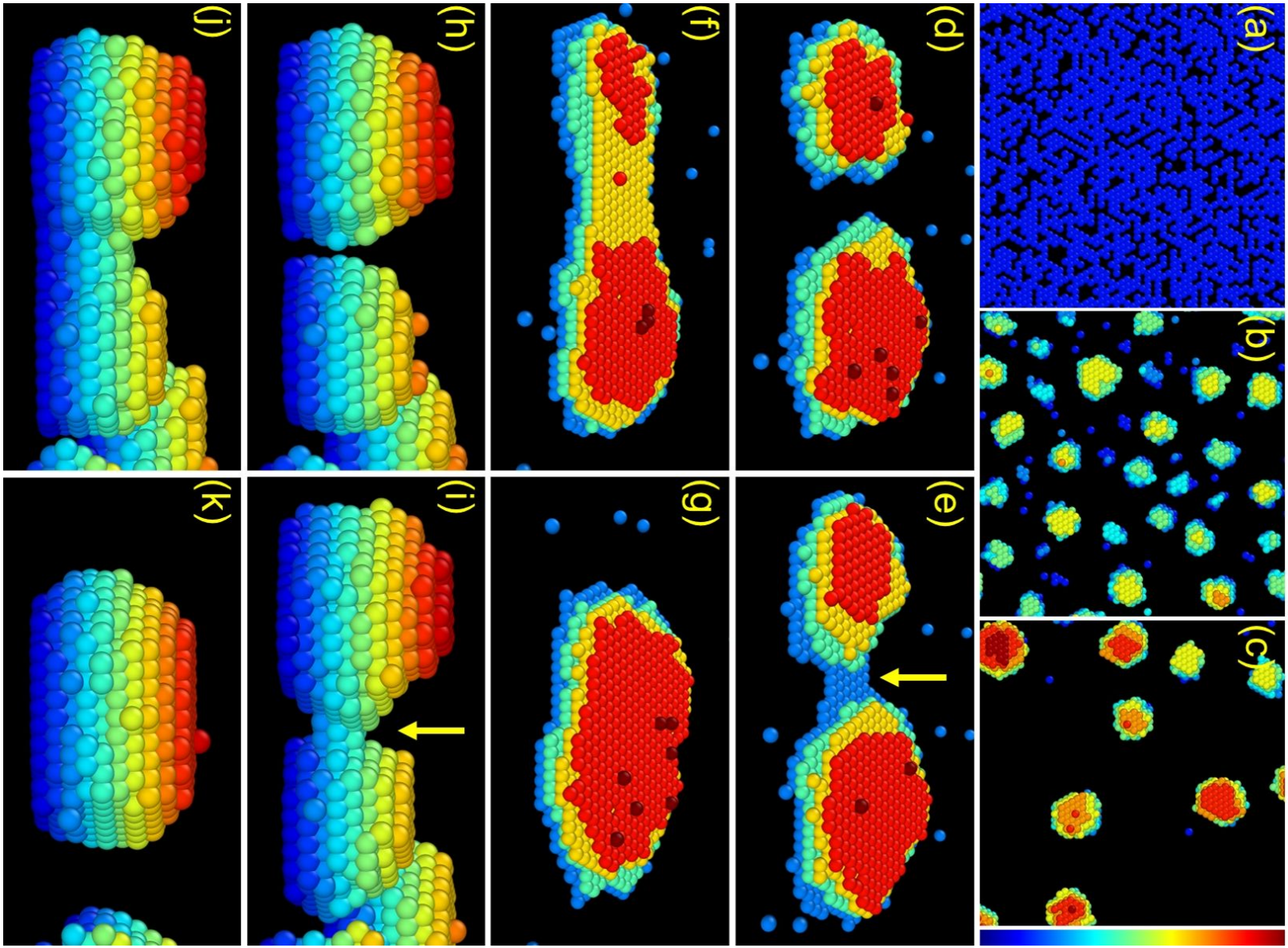

PLEASE CITE THIS ARTICLE AS DOI: 10.1063/5.0083139

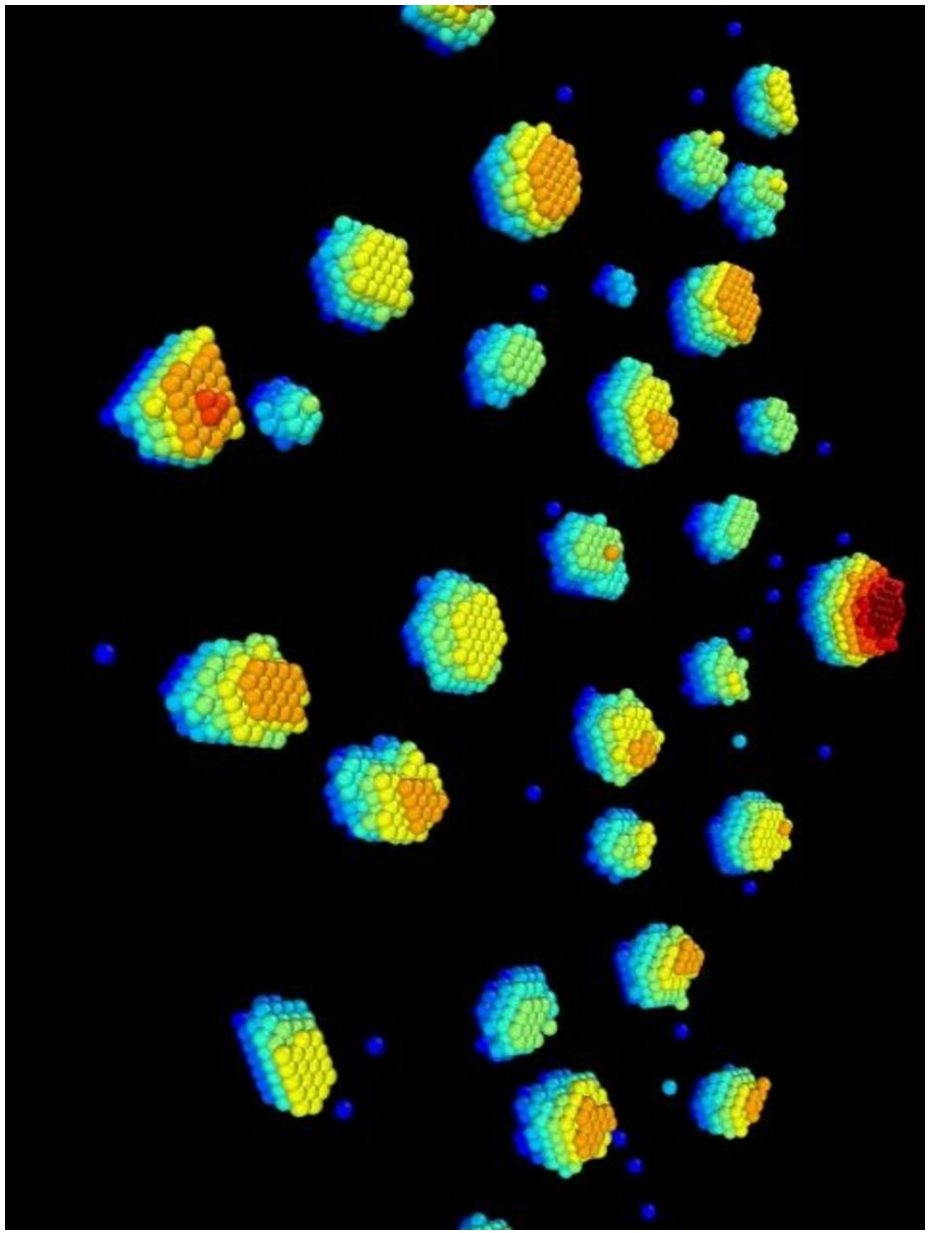

PLEASE CITE THIS ARTICLE AS DOI: 10.1063/5.0083139

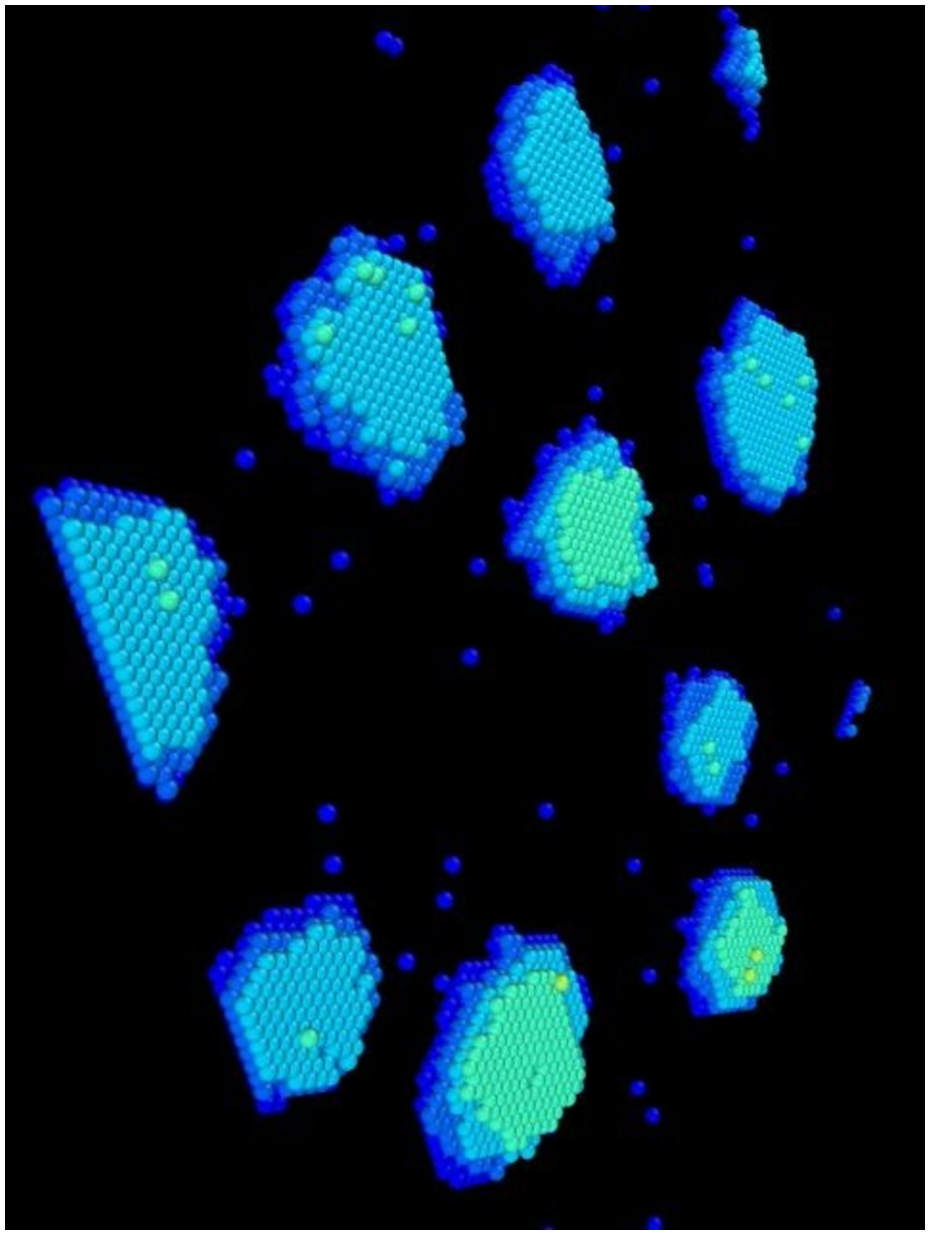

PLEASE CITE THIS ARTICLE AS DOI: 10.1063/5.0083139

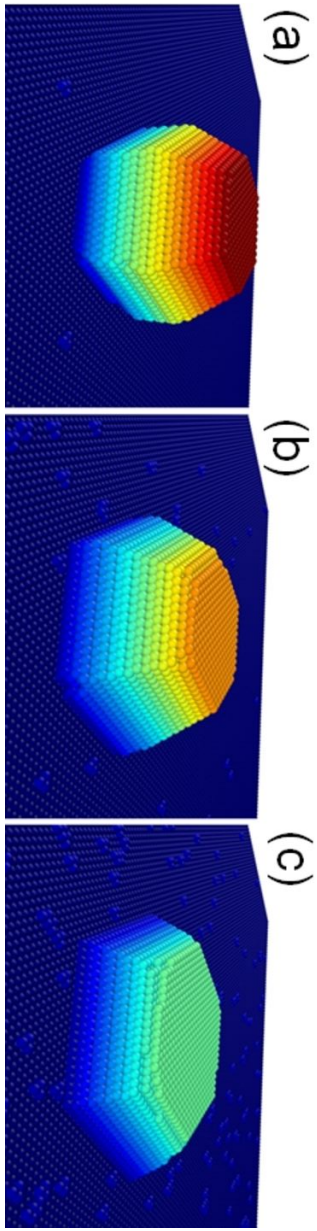

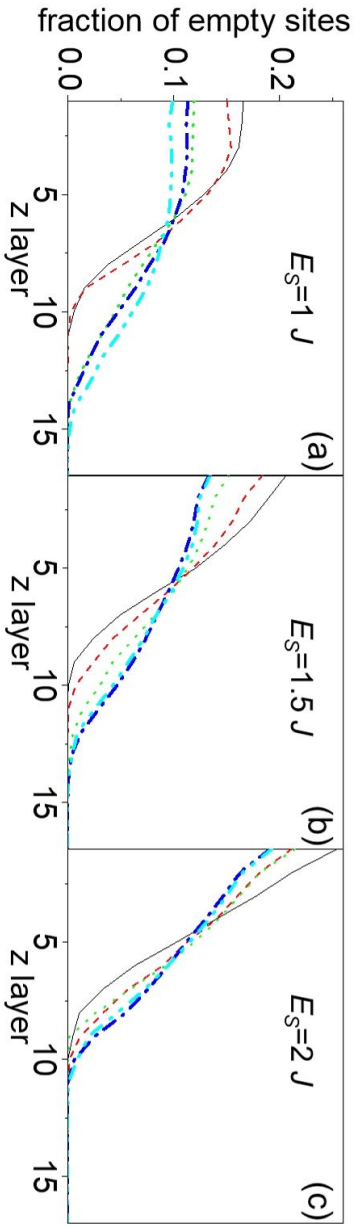

PLEASE CITE THIS ARTICLE AS DOI: 10.1063/5.0083139